ELSEVIER

Biochimica et Biophysica Acta 1457 (2000) 118–128

BIOCHIMICA ET BIOPHYSICA ACTA
BBA

www.elsevier.com/locate/bba

Morphological and functional changes of mitochondria from density separated trout erythrocytes

Luca Tiano [a,*], Patrizia Ballarini [a], Giorgio Santoni [b], Michal Wozniak [c], Giancarlo Falcioni [a]

[a] *Department of Biology MCA, University of Camerino, I-62032 Camerino (MC), Italy*
[b] *Department of Pharmacology and Experimental Medicine, University of Camerino, Camerino, Italy*
[c] *Department of Biochemistry, Medical Academic School, Gdansk, Poland*

Received 14 September 1999; received in revised form 4 January 2000; accepted 19 January 2000

Abstract

Density separated trout erythrocytes, using a discontinuous Percoll gradient, yielded three distinct subfractions (top, middle and bottom) since older cells are characterized by increasing density. Cells from each subfraction were incubated with mitochondria-specific fluorescent probe Mitotracker and JC-1 in order to assess mitochondrial mass and membrane potential by means of cytofluorimetric analysis, confocal microscopy and subsequent computer-aided image analysis allowing a detailed investigation at single cell level. Both cytofluorimetric data and image analysis revealed changes in size and redistribution of mitochondria starting from the light fraction to the bottom. In particular in young erythrocytes small mitochondria were detected localized exclusively around the nucleus in a crown-like shape, the middle fraction revealed enlarged mitochondria partially scattered throughout the cytosol, whereas the last fraction represented again mitochondria with reduced size being distinctly dispersed throughout the cytosol in the cells. Concerning membrane potential considerations, our study revealed a dramatic decrease of $\Delta\Psi_m$ in the bottom layer cell mitochondria compared to the top and unusual membrane potential increase of a subpopulation of enlarged mitochondria. ΔpH was also investigated in the three fractions by pretreating the cells with nigericin, allowing to confirm a mitochondrial energetic impairment in older cells.

Keywords: Trout erythrocyte; Mitochondria; Aging; Oxidative stress; Membrane potential; JC-1

1. Introduction

Aging is an inevitable biological process influenced by various factors, where oxygen free radicals are thought to be the most important, according to the theory proposed by Harman in 1956 [1–4]. The senescence process in human red blood cells (RBCs) has been extensively studied [5–7]. During their life span, RBCs undergo a series of changes involving both cytosolic and membrane molecular structures [8–10]. These age-related modifications could be due to oxidative stress deriving from the role in oxygen transport of these cells. However, information obtained by studying the aging process in these cells is limited by the fact that they are structurally simple, devoid of nucleus and mitochondria. Human RBCs may be separated into three/five populations by discontinuous density gradient [6,11], since older cells

* Corresponding author. Fax: +39 (737) 636216;
E-mail: l.tiano@cambio.unicam.it

0005-2728/00/$ – see front matter
PII: S0005-2728(00)00071-2

are characterized by increasing density. Using a similar technique, it is possible to separate the nucleated *Salmo irideus* trout erythrocytes in the range 45–65% Percoll, into three well-separated fractions. Previous studies demonstrated marked differences between human (anucleated) and trout (nucleated) density-separated erythrocytes. The activities of the primary antioxidant defense system made up of the enzymes superoxide dismutase, catalase and glutathione peroxidase increased in fish with the density of the fraction [12]. On the contrary, they decreased in density-separated human erythrocytes. Recently, using the 'Comet' assay, we examined DNA damage in whole and in density-separated trout erythrocytes and the results clearly showed that the degree of DNA damage increased with the density of the fraction [13]. Now, because of novel interest in mitochondrial research deriving from the unexpected role of mitochondria in the mechanism of apoptotic cell death [14–20], probably due to the possibility of mitochondria to be both the source and the final target of free radicals, we investigated the dimensions and energetic state of these organelles. The purpose of this study was to examine mitochondrial mass and membrane potential at single cell level during aging using different density-separated trout erythrocyte fractions. Cells from each fraction were incubated with mitochondria-specific fluorescent probes (Mitotracker and JC-1) and visualized by confocal microscopy, with subsequent computer-aided image analysis, and by flow cytometry. Mitotracker is a fluorochrome capable of selectively accumulate in mitochondria in an energy- and pH-independent manner [21–23], while JC-1 is a delocalized lipophilic cation which allows the analysis of changes in mitochondrial potential [24–28]. JC-1 is more advantageous over other potential-sensitive probes, such as rhodamines and other carbocyanines, since it changes its color from green to orange as the membrane potential increases (over values of about 80–100 mV). This property is due to the reversible formation of JC-1 aggregates upon membrane polarization that causes shifts in emitted light from 530 nm (i.e. emission of JC-1 monomeric form) to 590 nm (i.e. emission of J-aggregate).

Moreover by using nigericin, a ionophore which induces an electrically neutral exchange of protons for potassium ions and results in the elimination of the pH gradient across the mitochondrial membrane and a compensating increase in membrane potential, it was possible to follow in depth the energetics of the mitochondrion.

This investigation could be of interest for a better understanding of the molecular mechanisms involved in both the aging process and adaptation of aquatic organisms to their particular living conditions.

2. Materials and methods

All reagents were of analytical grade. Percoll and nigericin were purchased from Sigma (St. Louis, MO, USA); nigericin was solubilized in methanol as 2 mM stock solution and kept at 4°C until used. Fluorochromes Mitotracker and JC-1 were purchased from Molecular Probes (Eugene, OR, USA) and stored at −20°C as a 1 mM stock solution in DMSO.

2.1. Samples

The cells used in this study were obtained from *S. irideus*, an inbred strain of rainbow trout. The fish were kept in tanks containing water from Scarsito River and fed with commercial fish food. Experiments were performed on fish of the same age (approx. 24 months old), weighing between 180 and 300 g. Blood was withdrawn with a syringe from the lateral tail vein into an isotonic medium (0.1 M phosphate buffer, 0.1 M NaCl, 0.2% citrate, 1 mM EDTA, pH 7.8) and further treated within 2 h at 4°C. After removal of the plasma and buffy coat, the erythrocytes were washed three times with the same isotonic phosphate buffer. The erythrocytes were separated into three subpopulations on Percoll/BSA density gradient according to Rennie [29]. Suitable gradients lay in the range from 45 to 65% Percoll. The three fractions were collected and washed three times with isotonic phosphate buffer. Erythrocyte suspension from each subfraction was adjusted to a density of 1.3×10^5 cells/ml and incubated for 30 min at 35°C in the dark, with 400 μM Mitotracker for mitochondrial mass determination. For $\Delta\Psi_m$ assessment, the same amount of cells was incubated with 10 μg/ml of JC-1 for 10 min at room temperature in the dark. For $\Delta\mu H^+$ determination

cells were incubated with nigericin, at a 2 μM concentration, for 5 min before staining.

2.2. Flow cytometry

Briefly, a suspension of 1×10^6 cells/ml from each subfraction previously incubated with JC-1 was analyzed for relative fluorescence intensity using a FACScan flow cytometer (Becton Dickinson, Mountain View, CA, USA) equipped with a single 488 argon laser. The filter in front of the fluorescence 1 (FL1) photomultiplier transmits at 530 nm, and the filter used in the FL2 channel transmits at 585 nm. To better describe the variations in JC-1 fluorescence, for each histogram the median fluorescence channel was calculated. The values of photomultiplier (PMT) were logarithmically set. Green fluorescence (FL1) represents the monomeric form of JC-1, corresponding to mitochondrial mass. Red fluorescence (FL2) corresponds to the J-aggregate form of JC-1 and is proportional to $\Delta\Psi_m$. Compensation FL1-FL2 was 0.3%. A minimum of 13 000 cells per sample were acquired and analyzed using Consort 30 software on a Hewlett Packard 9000.

2.3. Confocal microscopy and Image analysis

After incubation, cell suspensions were washed in fresh buffer and a drop of suspension was spread onto a coverslip glass treated with L-polylysine prior to sealing. Samples were immediately analyzed with a Bio-Rad M600 laser-scanning confocal imaging system equipped with a krypton-argon laser and interfaced with a Nikon DIAPHOT-TMD inverted microscope mounting an objective apoplan 60× N.A. 1.4. To produce the double excitation, two excitation lines at 488 nm and 568 nm were used. The K1/K2 filter block set was used to separate emission into red and green bands. PMT and aperture were set to produce the brightest image possible against minimal background on a control sample; standard conditions were kept for all the measurements. Analysis was performed using the COMOS software package MPL program provided by Bio-Rad (Melville, NY, USA) on a single optical section through each sample. An optical section close to the middle of the cells in the *z*-plane was selected for analysis. Digital images in TIFF format (756×512×256) were processed using OSIRIS for Windows, an image analysis software developed from the University Hospital of Geneva. As different energetic states of mitochondria correspond to different concentrations of fluorochrome and thus different fluorescence intensity, under fluorescence microscopy imaging conditions, the analysis of the grey levels [30] of digital images of mitochondria allows the investigation of the energetic state of mitochondria in vivo at single organelle level. A region of interest (ROI) concerning a mitochondrial region was defined in order to avoid nonspecific fluorescence. Furthermore segmentation was performed in order to eliminate background fluorescence emission. Normalized grey scale frequency histograms relative to each ROI were calculated reporting the percentage of pixels showing the same

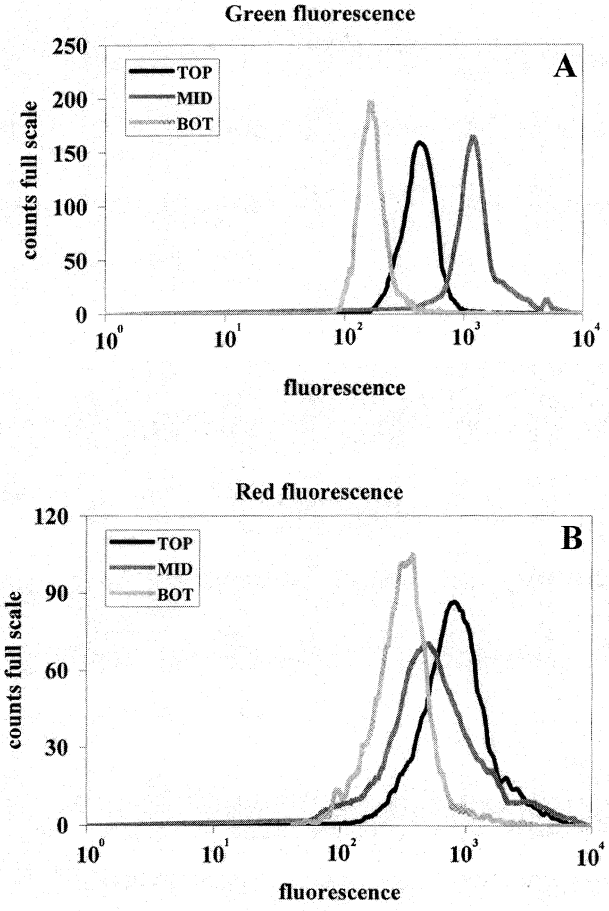

Fig. 1. Separate analysis of JC-1 fluorescence in flow cytometry of density-separated trout erythrocytes. Abscissa indicates fluorescence intensity, ordinate relative cell number. Green fluorescence (A) is proportional to mitochondrial mass, red fluorescence (B) is proportional to membrane potential.

intensity on the ordinate and the grey levels of fluorescence emission intensity on the abscissa. ROI for approx. 30 cells for every sample were analyzed, and mean frequency histograms were estimated. Alternatively, in order to better interpret the image analysis results, the data were further processed by clustering the grey levels in eight classes and evaluating the percentage of pixel in each class. Clusters 5–8 (grey levels 127–255) were referred to as 'bright region' and, in particular, cluster 8 (grey levels 223–255) was referred to as 'very bright region'.

3. Results

3.1. Flow cytometry

JC-1 green fluorescence (FL1) corresponding to mitochondrial mass, in erythrocytes from different subfractions, identified three well separated distribution histograms (Fig. 1A). In particular, erythrocytes from the middle subfraction turned out to possess the largest mitochondrial mass followed by the top and bottom fraction erythrocytes. Red fluorescence distribution (Fig. 1B) showed marked differences between top and bottom fraction erythrocytes indicating a remarkable decrease in the membrane potential of the latter.

Middle fraction erythrocytes exhibited a more heterogeneous distribution: despite the increase in mitochondrial mass/cell there was no significant increase in JC-1 red fluorescence in most middle fraction erythrocytes compared to those of the top fraction. The curves were largely overlapping indicating a constant summed mitochondrial potential, although a small subpopulation of cells exhibited the highest red fluorescence intensity. Considerations on mitochondrial mass and $\Delta\Psi_m$ were confirmed by calculation of the median fluorescence channel as reported in Fig. 2.

Cells from all the three subfractions after treatment with nigericin presented a significant increase in red fluorescence due to the conversion of the pH gradient across the mitochondrial membrane to an increase in membrane potential (Fig. 3). Top and middle fraction erythrocytes present a slightly bimodal distribution with the larger population of cells located in correspondence of high levels of fluorescence (Fig. 3A,B), whereas bottom fraction erythrocytes present a weaker emission (Fig. 3C). In conclusion the behavior indicated in $\Delta\Psi$ analysis is confirmed for $\Delta\mu H^+$, with younger cells presenting the highest fluorescence emission, followed by middle fraction erythrocytes that present a distribution largely overlapping with the previous and finally the oldest fraction erythrocytes located in cor-

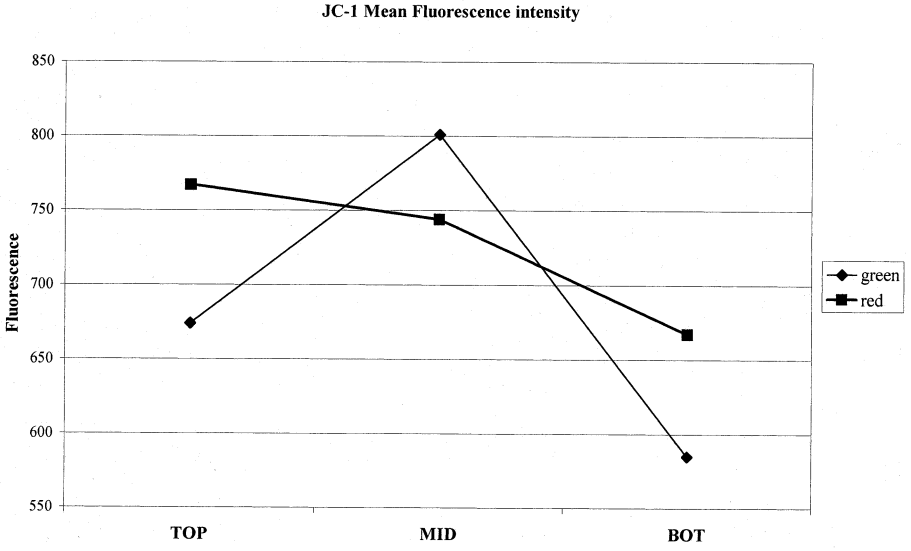

Fig. 2. Analysis of JC-1 fluorescence in flow cytometry of density-separated trout erythrocytes. Data are expressed as median fluorescence intensities. Data are referred to the experiment reported in Fig. 1.

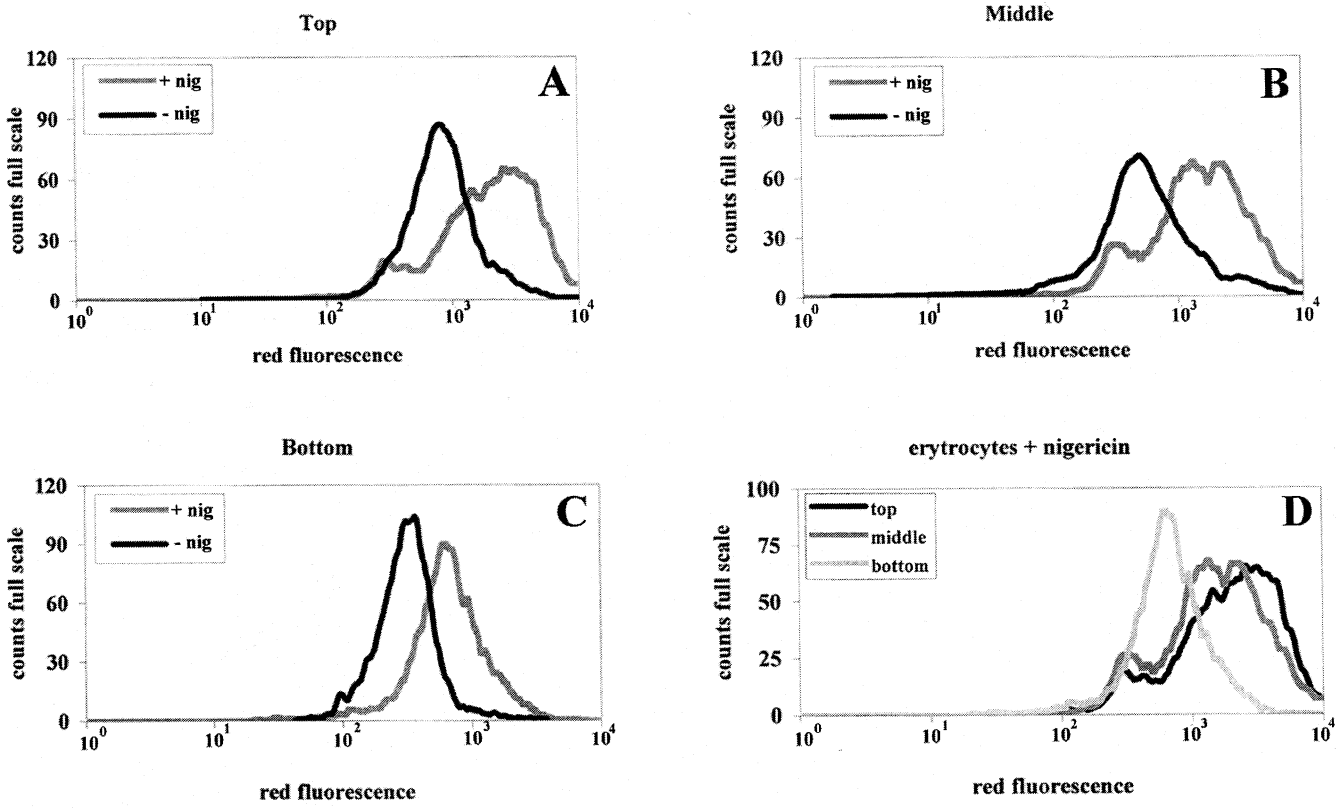

Fig. 3. Analysis of JC-1 red fluorescence, proportional to membrane potential, in flow cytometry of density-separated trout erythrocytes. Data for control samples and samples treated with nigericin are reported. Abscissa indicates fluorescence intensity, ordinate relative cell number. (A) Top; (B) middle; (C) bottom; (D) top, middle and bottom after treatment with nigericin.

respondence of lower values of fluorescence (Fig. 3D).

3.2. Cytochemical characterization

Staining with Mitotracker fluorochrome, in order to visualize mitochondrial mass, in different subfractions, led to the following results: in the top fraction the mitochondria resulted small, round-shaped, closely related and localized in a crown-like structure around the nucleus as displayed in Fig. 4A. In the middle fraction, mitochondria underwent a considerable enlargement and scattering in the cytosol as shown in Fig. 4C. Finally, in the bottom fraction, mitochondria were markedly reduced in shape and number (Fig. 4E). Localization of mitochondria is also visualized in the 3D reconstruction for top (Fig. 4B) and middle fractions (Fig. 4D), the small number of mitochondria in bottom fraction erythrocytes made the 3D reconstruction impossible. Concerning the membrane potential detected by means of JC-1 stain, images were acquired in both the red and green emission wavelengths characteristic of the monomeric form (corresponding to mitochondrial mass) and polymeric form (proportional to $\Delta\Psi_m$) of the probe, respectively. The top erythrocyte fraction displayed a strong emission in the red channel and high colocalization of the fluorescence, indicative of a considerable homogeneous activity of the mitochondria (Fig. 5A,B), whereas the middle fraction erythrocytes showed a heterogeneous fluorescence in the different channels. In particular, the enlarged mitochondria seemed to emit a considerable fluorescence in the red channel (Fig. 5D,E). Finally, in the bottom fraction, a dramatic fall in fluorescence in the red channel indicated a very low membrane potential in the older cells (Fig. 5G,H). Colocalization of fluorescence is detectable as yellow emission in Fig. 5C,F,I, representing the merged images from green and red channels.

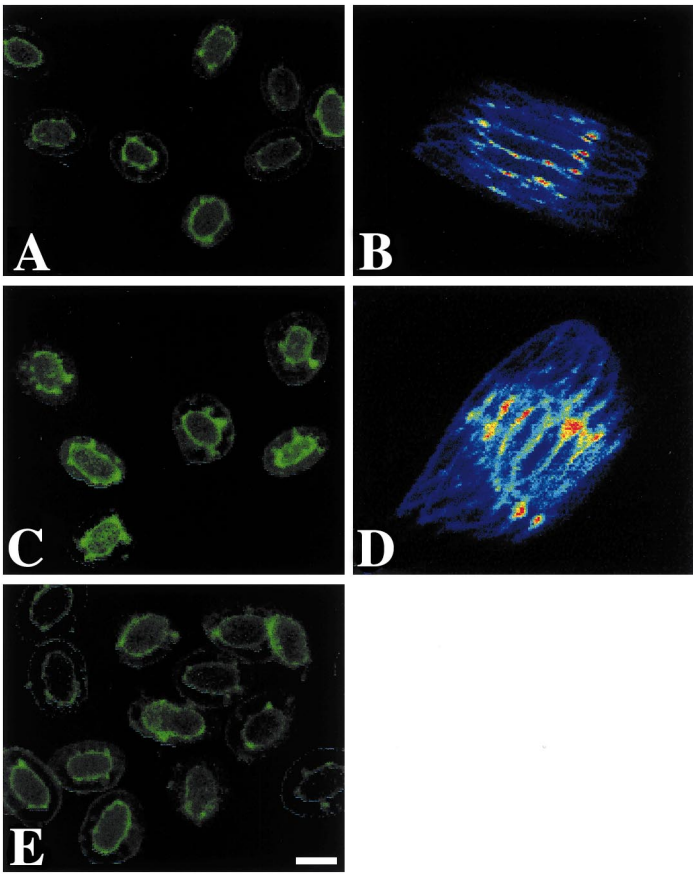

Fig. 4. Mitochondrial morphology analyzed by confocal microscopy using Mitotracker fluorochrome. Top (A), middle (C) and bottom (E) fraction erythrocytes are reported. Localization of mitochondria is better visualized in the 3D reconstruction for top (B) and middle (D) fractions. Pseudo-colors proportional to fluorescence intensity were applied to 3D reconstruction in order to better resolve mitochondrial position. Bar 10 μm.

3.3. Image analysis

The results obtained by confocal microscopy were confirmed by means of image analysis, which allows a semi-quantitative analysis of fluorescence emission at single cell level.

Grey scale frequency histograms of the red channel images relative to top and middle fraction erythrocytes presented a multimodal distribution of pixel (Fig. 6A,B), where two main populations could be identified: the main population of pixel centered on grey scale 90 and a smaller set of very bright pixel close to saturation. Both frequency distribution for the top and middle fractions where very comparable (approx. 40% of pixel in 'bright region' clusters 5–8, Fig. 6D) although the middle fraction distribution was not homogeneous. This was due to a subpopulation of cells exhibiting a marked increase of pixels in the very bright region (approx. 77% of pixels in 'bright region' clusters 5–8, of which 36% 'very bright' cluster 8, Fig. 6D). In the grey scale distribution of red channel images, from the bottom fraction erythrocytes, a marked increase of pixel below grey level 100 and an almost complete depletion of pixel in the 'bright region' were detectable (only 10% of pixel in 'bright region' clusters 5–8, 0% 'very bright' cluster 8, Fig. 6C,D), indicating a dramatic drop in $\Delta\Psi$ of the older cells as stated in flow cytometry. In order to reduce our field of investigation at single organelle level, we performed a segmentation of digital images using eight clusters of grey levels (Fig. 7) allowing the identification of mitochondrial areas presenting the same membrane potential. Fig. 7A shows mitochondria from younger cells which were

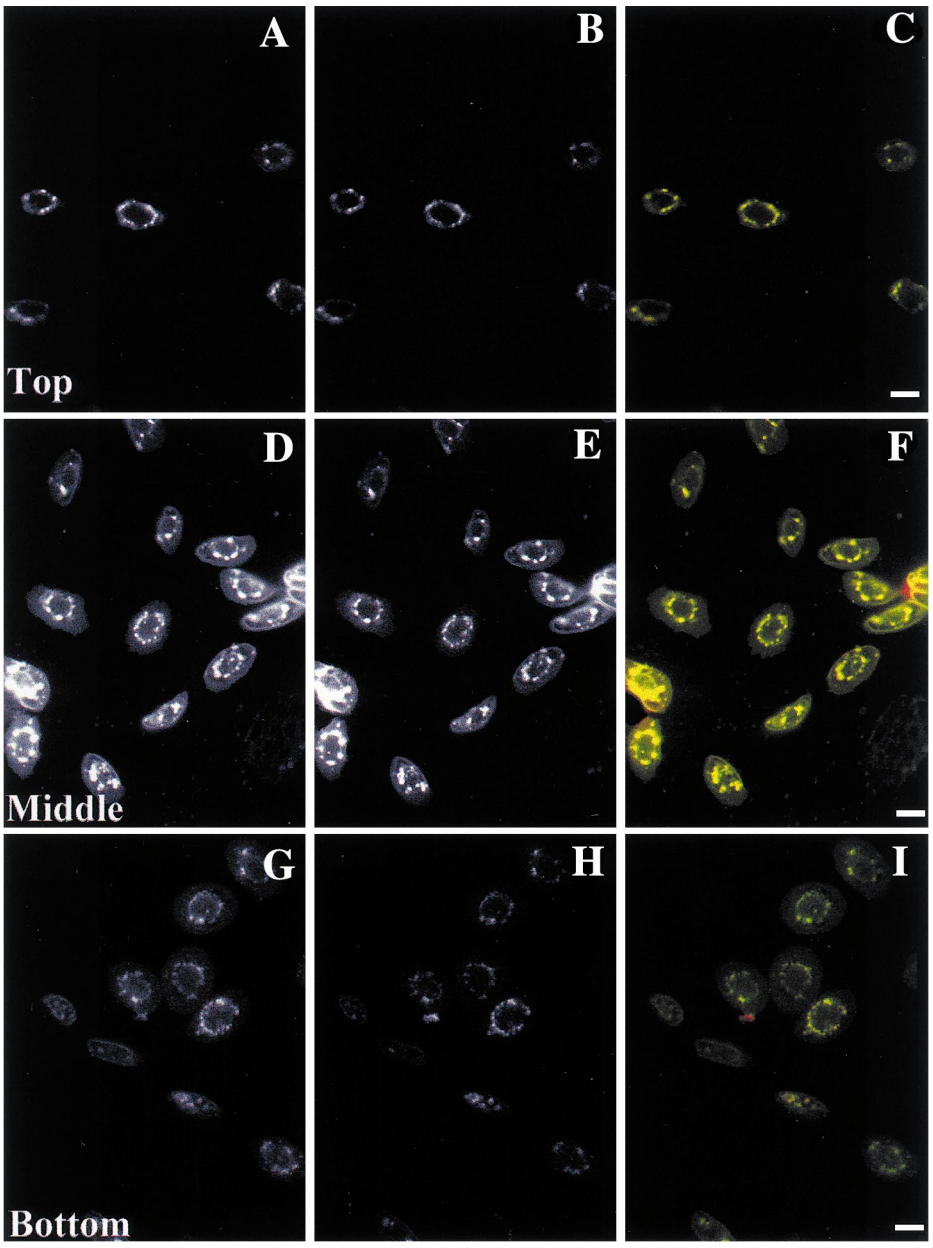

Fig. 5. Confocal micrographs of density-separated trout erythrocytes visualized with JC-1. Representative top (A,B,C), middle (D,E,F) and bottom (G,H,I) fraction erythrocytes. (Center) Red potential sensitive 590 nm emission; (left) green 527 nm emission; (right) merged channels. Bar 10 μm.

small but uniformly highly energized. Two fields were chosen for middle fraction erythrocytes because of the high variability of this fraction as reported in flow cytometry and image analysis (Fig. 7B,C). Both figures show enlarged mitochondria but the energetic state is very heterogeneous: uniformly energized mitochondria (Fig. 7B, ROI 10), coexistence of few energized mitochondria with the remaining deenergized population (Fig. 7C, ROI 7,5). In older erythrocytes only small mitochondria were detectable and most of the area presented low values of membrane potential (Fig. 7D).

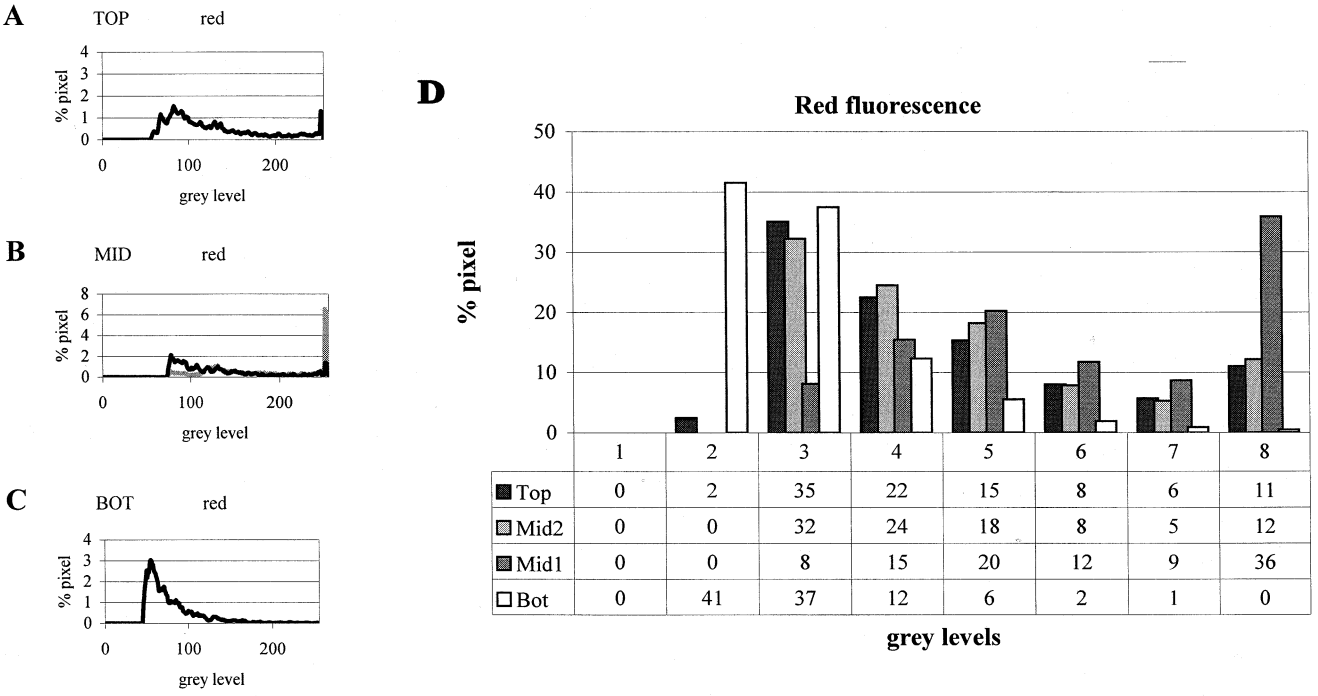

Fig. 6. Grey scale histogram of red channel images of density-separated trout erythrocytes stained with JC-1. Abscissa indicates grey levels (0–255) and ordinate relative percentage of pixels. (A) Top, (B) middle, and (C) bottom fraction erythrocytes. (D) Clustered representation of the same data. Each cluster represents 36 grey levels.

4. Discussion

It is known that there is a correlation between the density of erythrocyte subpopulation and aging [31,32]; older cells are characterized by an increased density. The present work was aimed at investigating the morphological and functional state of mitochondria in density-separated trout erythrocyte subpopulations. It is not possible to make analogous studies on human erythrocytes because these cells are devoid of mitochondria. It has been documented that during physiological development of mammal erythrocytes, mitochondria are eliminated by oxidative stress depending on the action of lipoxygenases, which disrupt mitochondrial membranes with consequent elimination of these organelles [33–36]. Using flow cytometry and confocal microscopy techniques, we obtained information on mitochondrial mass and membrane potential in individual cells. This approach has several advantages. Indeed, it is possible to analyze at single cell level potential variations, moreover in this way mitochondria can be studied in their physiological environment. The data presented here could suggest that the observed behavior might be due to different lengths of exposure of the density-separated fraction to the hazards of active oxygen radicals, with older cells (bottom layer) exposed to oxidative stress for a longer time. The improvement in the primary antioxidant defense system in older cells, by us previously reported [12], seems to be unable to protect DNA [13] and mitochondria while it could be efficient towards the lysis of the cell: it is important to point out that the rate of hemolysis is the same for the three erythrocyte fractions [12]. Our previous results support the participation of reactive oxygen species in the aging process of trout erythrocytes. In fact, we reported density-related differences in the antioxidant enzyme activities [12], in oxidative damage of cytosolic components [37] and oxidative damage to DNA [13]. It has also been shown that DNA damage was prevented by the presence of free radical scavengers, such as aromatic aminoxyls [38]. The data presented here and those previously reported are in agreement with the evolution theory which indicates that aging is caused by a progressive accumulation of

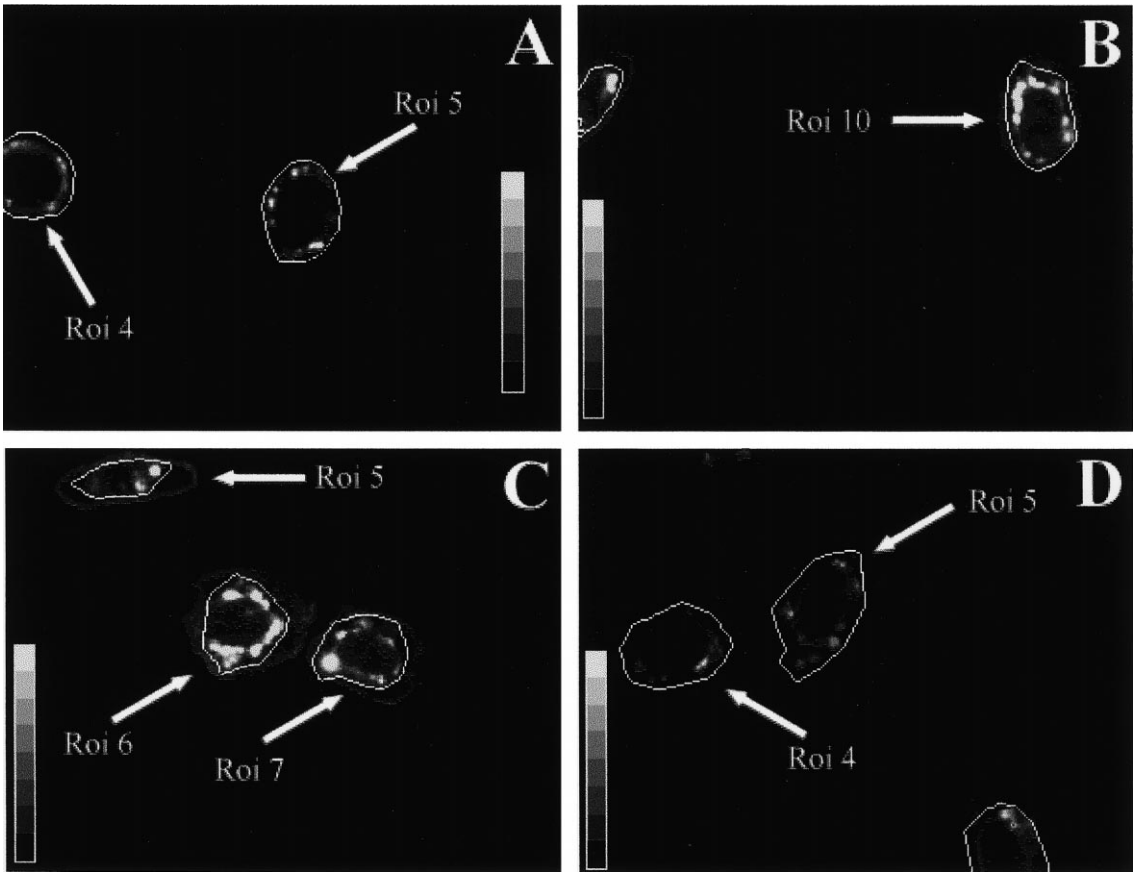

Fig. 7. Segmentation of red channel images of density-separated trout erythrocytes using eight clusters of grey levels. (A) Top, (B) middle, and (D) bottom fraction. (C) A sample (ROI 6.7) of energized swollen mitochondria.

defects and that multiple processes are operating in parallel [39]. The experimental data point out that mitochondria in nucleated trout erythrocytes are not remnants but instead can actively participate in the aging process. Our results highlight two main aspects of the age-related modifications of mitochondria.

(A) Mitochondria are subjected to marked changes in size and membrane potential, similarly to mitochondria from other cell types submitted to oxidative stress. In particular, after consistent swelling in the middle fraction, mitochondria undergo disrupture leading to fragmentation of organelles in the bottom fraction. Furthermore, age-dependent changes in bioenergetic capabilities are evident, they are confirmed by investigation of $\Delta\mu H^+$ by pretreating the cells with nigericin. Experiments with nigericin exclude the presence of compensatory effects: in our experimental model nigericin induced an increase in fluorescence in each subfraction but maintaining the same overall relative energetic trend.

(B) The unusual increase in membrane potential of a small population of enlarged mitochondria may be attributed to mitochondrial compensatory mechanisms. The loss of functional mitochondria with age could be compensated in part by the increased workload of the remaining intact population of mitochondria [2]. This hypothesis is supported by our investigation at single organelle level, as reported in Fig. 6C. In this figure ROI 7 has only one enlarged mitochondrion with high $\Delta\Psi_m$, while the remaining mitochondria show a consistent drop in potential. Besides the high membrane potential detected in these organelles it may not be not coupled with ATP synthesis. In fact, uncoupling has been hypothesized as a strategy for preventing or decreasing ROS production by mitochondria by enhancing oxygen consumption [40].

Finally these data, together with our previous results, indicating an increased formation of strand brakes in genomic DNA from erythrocytes of increasing age [13], raise the possibility of the involvement of a ROS-mediated apoptotic process in the aging of trout erythrocytes. Recently, it has been demonstrated that also cells with transcriptionally inactive nuclei (i.e. chicken erythrocytes) may undergo programmed cell death (PCD) [41]. In conclusion, trout erythrocytes could represent a good model for studying the kinetics of the different processes regarding the involvement of mitochondria in aging and in PCD.

Acknowledgements

The authors wish to thank Prof. Giorgio Lenaz for critical reading and helpful suggestions, and A.M. Santroni for skillful technical assistance.

References

[1] D. Harman, Aging, a theory based on free radical and radiation chemistry, J. Gerontol. 11 (1956) 298–300.
[2] M.K. Shigenaga, T.M. Hagen, B.N. Ames, Oxidative damage and mitochondrial decay in aging, Proc. Natl. Acad. Sci. USA 91 (1994) 10771–10778.
[3] R.S. Sohal, R. Weindruch, Oxidative stress, caloric restriction and aging, Science 273 (1996) 59.
[4] R. Weindruch, R.S. Sohal, Caloric intake and aging, New Engl. J. Med. 337 (1997) 986.
[5] A. Bovelli, M.A Castellana, G. Minetti, G. Piccinini, C. Seppi, M.R. De Renzis, C. Seppi, C. Balduini, in: Magnan and De Flora (Eds.), Red Blood Cell Aging, vol. 307, Plenum Press, New York, 1990, pp. 59–73.
[6] R. Fiorini, G. Curatola, A. Kantar, P.L. Giorgi, E. Bertoli, F. Tanfani, Steady state fluorescence polarization and Fourier transform infrared spectroscopy studies on membranes of functionally senescent human erythrocytes, Biochem. Int. 20 (1990) 715–724.
[7] S. Piomelli, C. Seaman, in: Magnan and De Flora (Eds.), Red Blood Cell Aging, vol. 307, Plenum Press, New York, 1990, pp. 105–113.
[8] G.J. Busmen, A. Anghersen, C.H. Vollard, K. Renkawek, I.G. Bartholomeus, A.M. Pistorius, K. Renkwek, W.J. De Grip, Implications in the aging and degeneration related changes in anion exchange for the maintenance of neuronal homeostasis, Cell. Mol. Biol. 42 (1996) 915–918.
[9] M. Gaczynska, Changes in proteolytic susceptibility of human erythrocytes membrane proteins during RBCs aging, Cytobiosis 72 (1992) 197–200.
[10] M.M. Kay, J.J. Marchalonis, S.F. Schulter, G. Bosman, Human erythrocyte aging: cellular and molecular biology, Transfus. Med. Rev. 5 (1991) 173–195.
[11] S.K. Jain, Evidence for membrane lipid peroxidation during the in vivo aging of human erythrocytes, Biochim. Biophys. Acta 937 (1988) 205–210.
[12] G. Falcioni, F. Grelloni, A.R. Bonfigli, E. Bertoli, Biochemical characterization of density-separated trout erythrocytes, Biochem. Int. 28 (1992) 379–384.
[13] M. Moretti, M. Villarini, G. Scasselati-Sforzolini, A.M. Santroni, D. Fedeli, G. Falcioni, Extent of DNA damage in density separated trout erythrocytes assessed by the 'comet' assay, Mutat. Res. 397 (1998) 353–360.
[14] A. Santos, N. Zamzami, G. Kroemer, Mitochondria as regulators of apoptosis: doubt no more, Biochim. Biophys. Acta 1336 (1998) 151–165.
[15] G. Lenaz, Role of mitochondria in oxidative stress and ageing, Biochim. Biophys. Acta 1366 (1998) 53–67.
[16] B. Mignotte, J.L. Vayssiere, Mitochondria and apoptosis, Eur. J. Biochem. 252 (1998) 1–15.
[17] V.P. Skulachev, Why are mitochondria involved in apoptosis? Permeability transition pores and apoptosis as selective mechanisms to eliminate superoxide producing mitochondria and cell, FEBS Lett. 397 (1996) 1–10.
[18] P.X. Petit, H. Lecoeur, E. Zorn, C. Daguet, B. Mignotte, M.L. Gougeon, Alterations in mitochondrial structure and functions are early events of hexamethasone-induced thymocyte apoptosis, J. Cell Biol. 130 (1995) 157–167.
[19] N. Zamzami, P. Marchetti, M. Castedo, C. Zanin, J.L. Vayssierie, P.X. Petit, G. Kroemer, Reduction in mitochondrial potential constitutes an early irreversible step of programmed lymphocyte death in vivo, J. Exp. Med. 181 (1995) 1661–1672.
[20] S. Camilleri-Broet, H. VanderWerff, E. Caldwell, H. Hockenbery, Distinct alterations of mitochondrial mass and function characterize different models of apoptosis, Exp. Cell Res. 239 (1998) 277–292.
[21] Y.Z. Zhang, Novel fluorescent acidic organelle-selective dyes and Mitochondrion-selective dyes that are well retained during cell fixation and permeabilization, Mol. Biol. Cell 5 (1994) 113–653.
[22] E. Vassella, K. Straessr, M. Boshart, A mitochondrion-specific dye for multicolor fluorescent imaging of *Trypanosoma brucei*, Mol. Biochem. Parasitol. 90 (1997) 381.
[23] D.L. Garner, C.A. Thomas, H.W. Joerg, J.M. DeJarnette, C.E. Marshall, Fluorometric assessment of mitochondrial function and viability in cryopreserved bovine spermatozoa, Biol. Reprod. 57 (1997) 1401.
[24] M. Poot, Y.Z. Zhang, J.A. Kraemer, K.S. Wells, L.J. Jones, D.K. Hanzel, A.G. Lugade, V.L. Singer, R.P. Haugland, Analysis of mitochondrial morphology and function with novel fixable fluorescent stains, J. Histochem. Cytochem. 44 (12) (1996) 1363–1372.
[25] S. Salvioli, A. Ardizzoni, C. Franceschi, A. Cossarizza, JC-1

but not DiOC6(3) or rhodamine 123, is a reliable fluorescent probe to assess $\Delta\Psi$ changes in intact cells. Implications for studies on mitochondrial functionality during apoptosis, FEBS Lett. 411 (1997) 77–82.
[26] S.T. Smiley, M. Reers, C. Mottola-Hartshorn, M. Lin, A. Chen, T.W. Smith, G.D. Steel, L.B. Chen, Intracellular heterogeneity in mitochondrial membrane potentials revealed by a J aggregate-forming lipophilic cation JC-1, Proc. Natl. Acad. Sci. USA 88 (1991) 3671–3675.
[27] M. Reers, T.W. Smith, L.B. Chen, J aggregate formation of carbocyanine as a quantitative fluorescent indicator of membrane potential, Biochemistry 30 (1991) 4480–4486.
[28] A. Cossarizza, M. Baccarani-Contri, G. Kalashnikova, C. Franceschi, A new method for the cytofluorimetric analysis of mitochondrial membrane potential using the J-aggregate forming lipophilic cation 5,5′,6,6′-tetrachloro-1,1′,3,3′-tetraethyl benzimidazol carbocyanine iodide (JC-1), Biochem. Biophys. Res. Commun. 197 (1993) 40–45.
[29] C.M. Rennie, S. Thompson, A.C. Parker, A. Maddy, Human erythrocyte fractionation in 'Percoll' density gradients, Clin. Chim. Acta 98 (1979) 119–125.
[30] P.H. Bartels, Numerical evaluation of cytologic data: description of profiles, Anal. Quant. Cytol. Histol. 1 (1979) 20–28.
[31] S. Piomelli, L. Lurinsky, L.R. Wasserman, The mechanism of red cell aging. I. Relationship between cell age specific gravity evaluated by ultracentrifugation in a discontinuous density gradient, J. Lab. Clin. Med. 69 (1967) 659–674.
[32] M. Rocchigliani, M. Pescaglini, S. Sestini, V. Micheli, C. Ricci, Density increase and aging of erythrocytes in stored blood, J. Intern. Med. Res. 17 (1989) 461–466.
[33] H. Kuhn, A.R. Brash, Occurrence of lipooxygenase products in membranes of rabbit reticulocytes. Evidence for a role of the reticulocyte lipooxygenase in the maturation of red cells, J. Biol. Chem. 265 (1990) 1454–1458.
[34] H. Kuhn, J. Belkner, R. Wiesner, Subcellular distribution of lipooxygenase products in rabbit reticulocyte membranes, in: J.R. Harris (Ed.), Blood Cell Biochemistry, vol. 1: Erythroid Cells, Plenum Press, New York, 1990, pp. 151–194.
[35] S.M. Rapoport, T. Schewe, B.-J. Thiele, Maturational breakdown of mitochondria and other organelles in reticulocytes, in: J.R. Harris (Ed.), Blood Cells Biochemistry, vol. 1: Erythroid Cells, Plenum Press, New York, 1990, pp. 151–194.
[36] T. Schewe, W. Halangk, C. Hiebsch, S.M. Rapoport, A lipooxygenase in rabbit reticulocytes which attacks phospholipids and intact mitochondria, FEBS Lett. 60 (1975) 149–152.
[37] R. Gabbianelli, A.M. Santroni, A. Concetti, A. Kantar, G. Falcioni, Superoxide anion handling by trout erythrocytes: a chemiluminescence study, Comp. Biochem. Physiol. 115C (1996) 83–87.
[38] M. Villarini, M. Moretti, E. Damiani, L. Greci, A.M. Santroni, D. Fedeli, G. Falcioni, Detection of DNA damage in stressed trout nucleated erythrocytes using the comet assay: protection by nitroxide radicals, Free Radic. Biol. Med. 24 (1998) 1310–1315.
[39] R.E. Pacifici, K.J.A. Davies, Protein, lipid, and DNA repair systems in oxidative stress. The free radical theory of aging revisited, Gerontology 37 (1991) 166–180.
[40] P.V. Skulachev, Role of uncoupled and non-coupled oxidations in maintenance of safely low levels of oxygen and its one-electron reductants, Q. Rev. Biophys. 29 (1996) 169–202.
[41] M. Weil, D.M. Jacobson, M.C. Raff, Are caspases involved in the death of cells with a transcriptionally inactive nucleus? Sperm and chicken erythrocytes, J. Cell Sci. 111 (1998) 2707–2715.